STRUCTURAL BEHAVIOR OF NORMAL AND HIGH-STRENGTH CONCRETE WALLS REINFORCED WITH GLASS FIBER-REINFORCED POLYMER BARS UNDER ECCENTRIC LOAD

Yaarub Gatia ABTAN [a], Hassan Falah HASSAN [a*]

[a] Assistant Prof. PhD; Civil Engineering Department, Al-Mustansiryah University, Baghdad, Iraq
*E-mail address: *hassanfala@gmail.com*

Received: 22.09.2016 ; Revised: 5.02.2017; Accepted: 17.03.2017

Abstract

The solution of using glass fiber reinforced polymer (GFRP) bars, as reinforcement in concrete structures to overcome the problems created by steel corrosion, is now widely accepted because of both its non-corrosive nature and good results shown by large investigation efforts. In this paper twenty tests had been conducted on reinforced concrete wall specimens of (800 mm height x 450 mm width x 50 or 70 mm thickness effective dimensions). Four specimens were reinforced with steel bars to be considered as references, while the others were reinforced with GFRP bars. The specimens were made using normal and high strength concrete. All specimens showed similarity in the structural behavior and load pattern, the results show that Steel reinforced walls have 28% higher ultimate load than corresponding GFRP reinforced walls, also an approximate linear increase in the failure load with increasing in flexural GFRP reinforcement in range from 40.4% to 98.8% for NSC walls and in range of 70% to 115.1% for HSC walls. The ductility of the specimen reinforced with GFRP bars is 46% higher than that of steel reinforced specimens.

Streszczenie

Zastosowanie prętów z włókien szklanych (GFRP) jako zbrojenia w konstrukcjach betonowych, w celu uniknięcia problemów związanych z korozją stali, stało się obecnie popularne z uwagi na brak korozji jak i dobre wyniki wielu badań. W tym artykule przedstawiono 20 badań elementów ściennych, żelbetowych (o następujących wymiarach: wysokości 800 mm, szerokości 450 mm i grubości 50 lub 70 mm). Cztery elementy próbne zostały zazbrojone prętami stalowymi i stanowiły element porównawcze, a pozostałe zostały zazbrojone prętami GFRP. Elementy próbne zostały wykonane z betonu zwykłego (NSC) i o podwyższonej wytrzymałości (HSC). Wszystkie elementy wykazały podobieństwo w pracy pod obciążeniem. Wyniki badań wykazały, że ściany zbrojone stalą wykazywały 28% większą nośność przy zniszczeniu w stosunku do odpowiadających ścian zbrojonych GFRP. Jednocześnie uzyskano w przybliżeniu liniowy przyrost wartości obciążenia niszczącego przy zginaniu, w miarę zwiększania zbrojenia GFRP, w przedziale od 40,4% do 98,8% dla ścian NSC i w przedziale od 70% do 115.1% dla ścian HSC. Ciągliwość elementów zbrojonych GFRP była 46% wyższa niż elementów zbrojonych stalą.

Keywords: **Walls; GFRP Reinforcement; High Strength Concrete; Ductility; Concrete Structures.**

1. INTRODUCTION

Nowadays, using high strength concrete is widely spread in compression members than in flexural members those are mainly controlled by deflection criteria. Concrete walls are of vital priority among the remaining structural elements, therefore their concrete and steel durability, protection against deterioration and degradation are of paramount importance for safety issues. Continuous trials, to improve the quality and performance of such members had been conducted on concrete, by using additives and different types of fibers to produce more firm matrices, and on reinforcement by replacing the traditional steel bars by the GFRP bars to eliminate the problem of steel corrosion which disintegrate the surrounding concrete due to volume change of corroded steel [1].

GFRP is a nontoxic material, with low hazard impact to human and environment can be used in concrete structures instead of the traditional steel reinforcement, the most important feature of GFRP is that its coefficient of thermal expansion is similar to that of concrete, which prevents cracking under temperature changes.

Although FRPs are materials with high tensile strength and exhibit a linearly elastic stress strain relationship until failure without any plastic behavior (yielding), but their anisotropic properties oriented the researches test done by (Mallick 1988,Wu 1990, Ehsani 1993) [1] to support the reliability of GFRP bars to resist the compressive stresses, which conclude to that the compressive elastic modulus, of GFRP and CFRP (50-60% fiber volume), is 80% and 85% of its tensile modulus of elasticity and the compressive strength is 55%, 78% of the tensile strength respectively.

Reinforced concrete walls are widely used as structural elements in locations where they are subjected to axial loads and end moments, and appear as integral components in box frames, folded plates, box girders, box culverts, tee beams, etc. [2].

In the past, concrete walls were designed in most structures for protection against the

external environmental conditions with little consideration for the capability of the wall as a structural member. This approach was mainly due to the very low allowable design stresses for walls specified in early versions of published concrete codes.

Over the years, reinforced concrete walls have gained greater acceptance, by practicing engineers, as load-carrying structural members. This acceptance is due to the increased research undertaken on concrete walls and the subsequent increase in allowable design stresses incorporated in various current concrete codes [3].

2. RESEARCH SIGNIFICANCE

This experimental study aimed to explore the mechanical behavior of the high strength concrete walls reinforced with GFRP bars under eccentric load.

3. EXPERIMENTAL PROGRAM

This paper presents an experimental study to investigate the behavior of eccentrically loaded reinforced concrete walls reinforced with GFRP bars and compared to walls of traditional steel reinforcement, the specimens were denoted by (G or S) which stands for GFRP and steel, then by (H or N) for high and normal strength concrete, then by 1, 2, 3 and 4 for reinforcement ratio (ρ), then by 5 or 7 which are wall thickness.

3.1. Walls specimens

Total of twenty reinforced concrete walls were tested to failure to assess the performance of the GFRP bars with normal and high strength concrete compared to traditional deformed steel bars, four specimens (denoted by letter S for steel) were cast with normal and high strength concrete, all the remaining sixteen wall specimens (denoted by G for GFRP bars) were cast with normal and high strength concrete reinforced with different reinforcement ratio, Table 1 shows specimens designation and test program matrix.

Table 1.
Test Program Details

Specimen	Type of Reinforcement	$^*\rho$	Wall Thickness (mm)	$f'c$ (MPa)
SN-1-5	Steel	0.0048	50	30
SN-1-7	Steel	0.0032	70	30
SH-1-5	Steel	0.0048	50	72
SH-1-7	Steel	0.0032	70	72
GN-1-5	GFRP	0.0048	50	30
GN-2-5	GFRP	0.0074	50	30
GN-3-5	GFRP	0.0096	50	30
GN-4-5	GFRP	0.012	50	30
GN-1-7	GFRP	0.0032	70	30
GN-2-7	GFRP	0.0049	70	30
GN-3-7	GFRP	0.0064	70	30
GN-4-7	GFRP	0.008	70	30
GH-1-5	GFRP	0.0048	50	72
GH-2-5	GFRP	0.0074	50	72
GH-3-5	GFRP	0.0096	50	72
GH-4-5	GFRP	0.012	50	72
GH-1-7	GFRP	0.0032	70	72
GH-2-7	GFRP	0.0049	70	72
GH-3-7	GFRP	0.0064	70	72
GH-4-7	GFRP	0.008	70	72

All walls were reinforced with 6mm GFRP and steel bars with different spacing as shown in Figures 1 and 2, walls have the same over all dimensions 800×450×50 or 70 mm.

Figure 1.
Reinforcing details

Figure 2.
Test Specimens

3.2. Testing

3.2.1. Testing machine

The main testing machine is a universal testing machine (8551 M. F. L. system) available in the Structural Laboratory in Civil Engineering Department College of Engineering of AL-Mustansiryia University as shown in Figure 3. The panels are tested by this machine after making some arrangement to simulate the support condition for the panels. The concrete prisms and cylinders were tested by the same machine to measure the tensile and compression strength of concrete.

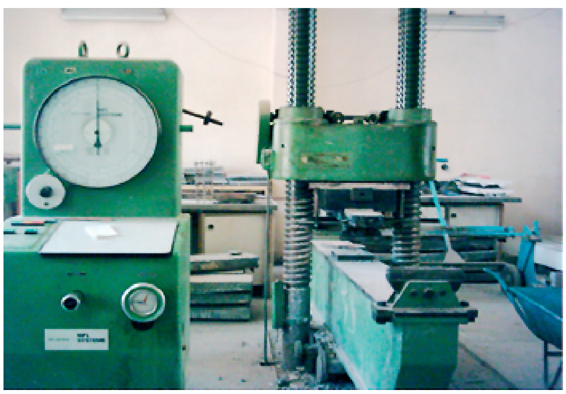

Figure 3.
Testing Machine

3.2.2. Test rig set-up

The test rig in the case of axially loaded walls (hinged at top and bottom) must satisfy two main conditions. Firstly, the supports of the wall panel to be tested must be allowed to rotate freely, while at the same time they should not move or deflect laterally. Secondly, the axial load must be uniformly distributed across the length of the test panel at a certain eccentricity [4]. Based on the previous researches used test rigs,and in order to make a simple, economical and functional test rig (support simulation), it has been seen that the best one for our study was the test rig used by [5]. With some amendments to the test rig used by Swartz, et al (1974) [5], each top and bottom hinged support conditions is simulated by attaching a 32 mm diameter high strength steel rod on a channel of size (C50 mm×3 kg/m) and welded very well for a length of rod and channel 1.0 m to ensure that the panels will be within the length of the channel. Two high strength steel rods of 12 mm then attached and welded very well to either flange of I-steel section to make a suitable guide for the steel rod of 32 mm that attached to the channel.

In order to satisfy the eccentricity when the loading is applied, the concrete panels restrained with a series of screws fixed on one side at the top and bottom channel. These screws could be adjusted for various eccentricities. Details of the simply supported top hinged edge are shown in Figures 4 and 5. The two I-sections fixed to the test machine by many clamps tightly, top and bottom taking care with the straightening of the two I-sections. After the test rig has been fixed, the panel fixed to the top and bottom hinge supports, leveling the panel to ensure the perpendicularity of the panel and then tightening the screws to satisfy eccentricity and also fixing the panel, and applying the load to the failure of the panel. Figure 5 shows these arrangements.

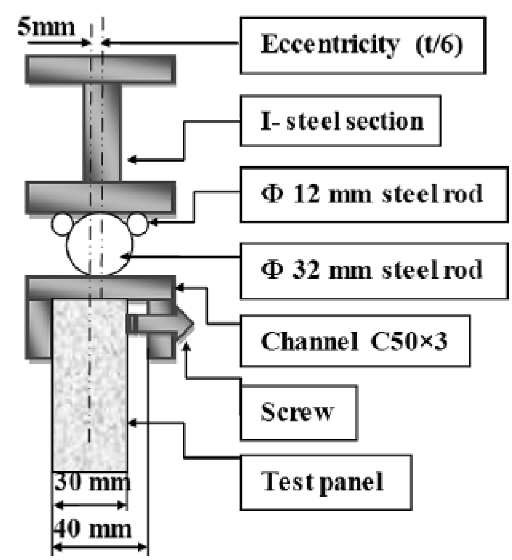

Figure 4.
Details of Supports Used in Tests

3.3. Materials

The high strength concrete used throughout this research was made from Portland cement type I comply with Iraqi standard no. 5/1984, crashed coarse aggregate with a specific gravity 2.65 and maximum nominal size 10 mm, and fine aggregate sand with specific gravity 2.66 and fineness modulus 3. Modified polycarboxylate based polymer superplasticizer admixture in a dose of 3 to 4% by weight of cement was added to mixing water to achieve the required workability.

Implementing the ACI mix design procedure, the final proportions of the mixes with a stiff plastic slump were achieved for the required compressive strength as in Table 2.

Figure 5.
Supporting Elements

Table 2.
Mix Proportions

Mix Type	Cement kg/m³	Coarse Aggregate kg/m³	Fine Aggregate kg/m³	Water kg/m³	Super-plasticizer L/m³
NSC	400	800	1200	200	---
HSC	525	1108	685	157	18

The characteristic strength values Table 3 were determined using standard cylinders of (100×200 mm and 150×300 mm) and prisms of (100×100×300 mm) and tested by a calibrated testing machine as per the standard testing ASTM procedures.

Table 3.
Properties of Hardened Concrete

Concrete Type	$f'c$ (MPa)	Target Concrete Strength(MPa)	f_r (MPa)	f_t (MPa)
NSC	30	32	3.6	3.3
HSC	72	75	8	7.5

The main relevant properties of both types of reinforcement used in the study are listed in Table 4.

Table 4.
Properties of Steel, GFRP Reinforcement*

FEATURE	STEEL	GFRP
Density g/cm³	7.8	2
Tensile strength MPa	fy=460	fu=1200
Modulus of Elasticity MPa	200000	55000
Equivalent Replacement Rebar Φ mm	10	6
Coefficient of Thermal Expansion α x10^{-6}/C°	11.7	6-10

*By manufacturer

4. EXPERIMENTAL RESULTS AND DISCUSSION

4.1. Failure mode and strength

In general, and regardless the types of either the longitudinal or transverse reinforcement, the modes of failure were same for all the twenty specimens. With the increase of load the lateral deformation at the mid height section increase toward the tension side, which accompanied with the appearance of the first transverse crack, tension failure occurs after excessive widening of the crack and increase in the curvature of the specimen. This similarity in behaver under load indicates that crack pattern and tension failure modes were not affected by the reinforcement type. Test results, Table 6, show variable % (average 28%) increase of ultimate load of steel reinforced specimens than the corresponding GFRP reinforced ones, also the ratios of the first crack load to ultimate load are in the range of 0.15 with a slight increase with the increase in main reinforcing ratio.

Table 5.
Lateral Displacements Corresponding to Ultimate and Crack Load

Specimens	First Crack Load P_c (kN)	Lateral Deform-ation Δ_c (mm)	Ultimate Load P_u (kN)	Lateral Deform-ation Δ_u (mm)	P_c/P_u	Δ_u/Δ_c
SN-1-5	13	0.54	85	5.44	0.15	10
SN-1-7	16	0.8	98	8.3	0.16	10
SH-1-5	18	0.31	108	4.57	0.17	15
SH-1-7	26	0.45	150	7.22	0.17	16
GN-1-5	9	0.22	52	3.44	0.17	16
GN-2-5	11	0.37	57	2.78	0.19	8
GN-3-5	13	0.22	67	4.60	0.19	21
GN-4-5	14	0.6	73	7.96	0.19	13
GN-1-7	13	0.5	81	7.01	0.16	14
GN-2-7	15	0.49	95	10.82	0.16	22
GN-3-7	18	0.63	130	11.48	0.14	18
GN-4-7	19	0.77	161	10.78	0.12	14
GH-1-5	14	0.4	86	8.78	0.16	22
GH-2-5	18	0.6	105	10.39	0.17	17
GH-3-5	25	0.49	137	11.38	0.18	23
GH-4-5	31	0.56	185	8.91	0.17	16
GH-1-7	15	0.43	145	10.98	0.1	26
GH-2-7	20	0.5	190	11.5	0.1	23
GH-3-7	26	0.52	225	9.92	0.12	19
GH-4-7	33	0.62	245	13.44	0.13	22

4.2. Flexural GFRP reinforcement

When increasing (ρ) from (0.0048) to (0.012) the ultimate load capacity increased by (40.4%), and by (98.8) for NSC walls with 70mm thickness, respectively.

On the other hand, the ultimate load was increased by 115.1% and 70% for the HSC-wall of 50 and 70 mm thickness, respectively. Figure 6 shows the effect of increasing the reinforcement ratio on the ultimate load.

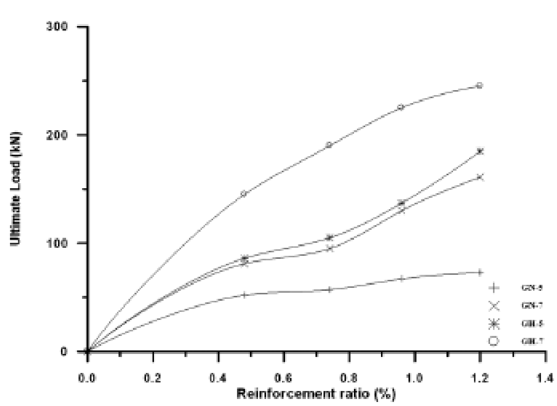

Figure 6.
Influence of Reinforcing Ratio on Ultimate Load

4.3. Wall thickness

The ultimate load capacity increases with the increasing wall thickness; Table 6 shows the effect of increasing walls thickness from 50 to 70 mm on first crack and ultimate loads. It can be seen that the increasing percentages for walls reinforced by GFRP bars are higher than walls reinforced by traditional steel reinforcement.

Table 6.
Effect of Increasing Wall Thickness on Ultimate and Crack Load

Specimen	First Crack Load P_c (kN)	Increasing %	Ultimate Load P_u (kN)	Increasing %
SN-1-5	13	23	85	15.3
SN-1-7	16		98	
SH-1-5	18	44.4	108	38.9
SH-1-7	26		150	
GN-1-5	9	47	52	55.7
GN-1-7	13		81	
GN-2-5	11	36.4	57	66.7
GN-2-7	15		95	
GN-3-5	13	38.5	67	94
GN-3-7	18		130	
GN-4-5	14	35.7	73	120.5
GN-4-7	19		161	
GH-1-5	14	7	86	68.6
GH-1-7	15		145	
GH-2-5	18	11	105	81
GH-2-7	20		190	
GH-3-5	25	4	137	64.2
GH-3-7	26		225	
GH-4-5	31	6.5	185	32.4
GH-4-7	33		245	

4.4. Concrete compressive strength

Generally, the ultimate load capacity increases with the increasing concrete compressive strength. The ultimate load in walls with 50 mm thickness increased by average 102.1%, and by average 76.1% for walls with 70mm thickness when ($f'c$) increasing from 30 to 72 MPa. Table 7 shows the effect of compressive strength on ultimate load.

4.5. Load displacement behavior

The curves, relating applied load to lateral displacement, are shown in Figures 2, 3, 4 and 5. All specimens reinforced with GFRP bars exhibit linear deformation response to the applied load at first stage, then a more inclined curve with a decreasing slope till failure. The curves did not show distinct yield point or a clear plastic range like those of specimens reinforced with steel bars. This is because the difference in behavior of GFRP bars, which do not possess a yield point in their stress strain behavior curve, com-

Table 7.
Effect of Increasing in Concrete Compressive Strength on Ultimate and Crack Load

Specimen	First Crack Load P_c (kN)	Increasing %	Ultimate Load P_u (kN)	Increasing %
SN-1-5	13	38.5	85	27
SN-1-5	18		108	
SH-1-7	16	62.5	98	53
SH-1-7	26		150	
GN-1-5	9	55.6	52	65.4
GN-1-5	14		86	
GN-2-5	11	63.6	57	84.2
GN-2-5	18		105	
GN-3-5	13	92.3	67	104.5
GN-3-5	25		137	
GN-4-5	14	121.4	73	153.4
GN-4-5	31		185	
GH-1-7	13	15.4	81	79
GH-1-7	15		145	
GH-2-7	15	33.3	95	100
GH-2-7	20		190	
GH-3-7	18	44.4	130	73.1
GH-3-7	26		225	
GH-4-7	19	73.7	161	52.2
GH-4-7	33		245	

paring to steel bars. Specimens reinforced with traditional steel give higher ultimate load (average 20%) with lower displacement (average 21%) than the corresponding specimens reinforced with GFRP bars due to higher modulus of elasticity of steel.

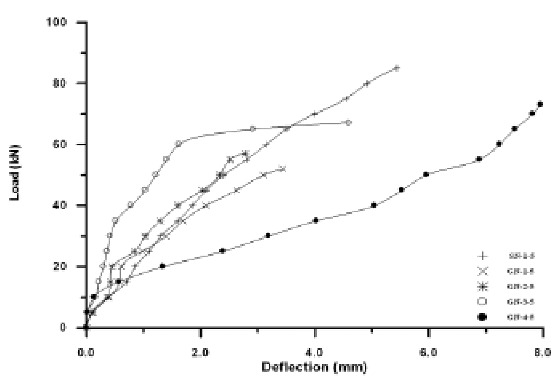

Figure 7.
Load-Deflection Curves for NSC Specimens with 50 mm Thickness

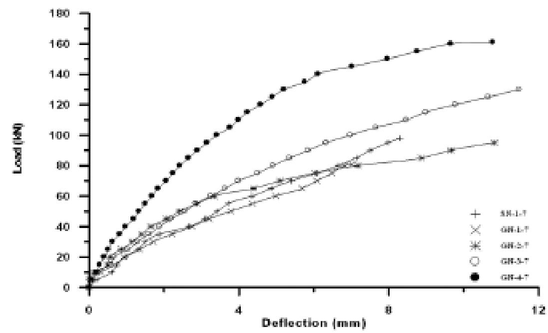

Figure 8.
Load-Deflection Curves for NSC Specimens with 70 mm Thickness

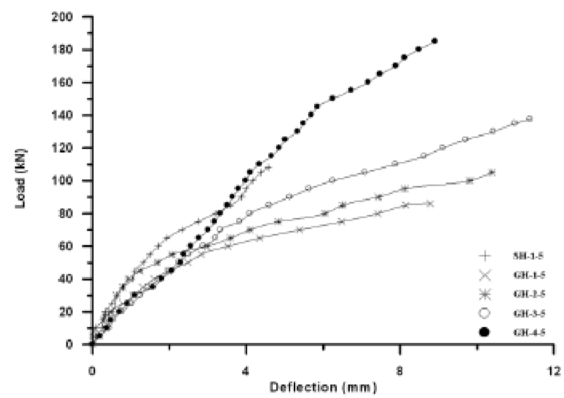

Figure 9.
Load-Deflection Curves for HSC Specimens with 50 mm Thickness

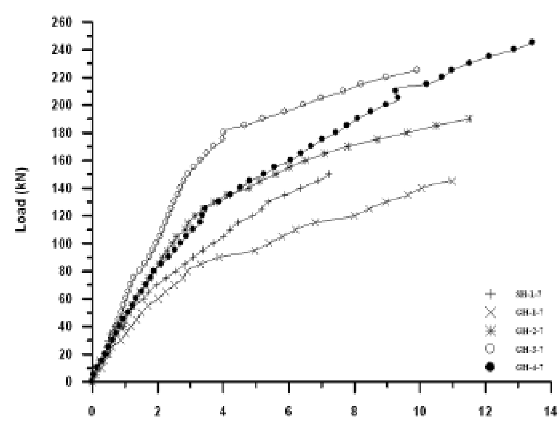

Figure 10.
Load-Deflection Curves for HSC Specimens with 70 mm Thickness

4.6. Ductility

Ductility in a structural member means the maintaining of strength while sizeable deformation or deflection occurs. Physically it is the warning of overload presence in the form of excessive cracking and deflection. Many researchers [6, 7, 8, 9] define ductility ($\mu_u = \Delta_u/\Delta_y$) as a ratio based on the deflection of the member at yield of reinforcement, which can be seen clearly at the beginning of the nearly horizontal part of the load deflection curves (the plastic plateau), and since the GFRP reinforcing bars have no yield stress point and behave elastically till failure, the first crack deflection can be considered as a base to compare ductility of member as ($\mu = \Delta_u/\Delta_c$). Table 8 shows that walls reinforced with steel bars exhibit less ductility than those reinforced with GFRP of same reinforcing ratio by 60 and 40% for NSC walls with 50 and 70 mm thickness, respectively.

Experimental results show also that the increasing concrete compressive strength from 30 to 72 MPa leads to increase in ductility by average 45.6% for walls with 50 mm thickness, and by average 40% for 70 mm wall thickness as shown in Table 9.

On the other hand Table 10 shows that the increase in GFRP reinforcement ratio leads to decrease in ductility by average 9.4 and 27.1% for NSC and HSC walls, respectively.

Table 8.
Effect of Reinforcement Type on Ductility

Specimen	Reinforcement Type	Δ_u/Δ_c	Increasing %
SN-1-5	Steel	10	60
GN-1-5	GFRP	16	
SN-1-7	Steel	10	40
GN-1-7	GFRP	14	

Table 9.
Effect of Concrete Compressive Strength on Ductility

Specimen	$f'c$ (MPa)	Δ_u/Δ_c	Increasing %
SN-1-5	30	10	50
SH-1-5	72	15	
SN-1-7	30	10	60
SH-1-7	72	16	
GN-1-5	30	16	37.5
GH-1-5	72	22	
GN-2-5	30	8	112.5
GH-2-5	72	17	
GN-3-5	30	21	9.5
GH-3-5	72	23	
GN-4-5	30	13	23
GH-4-5	72	16	
GN-1-7	30	14	85.7
GH-1-7	72	26	
GN-2-7	30	22	4.5
GH-2-7	72	23	
GN-3-7	30	18	12.5
GH-3-7	72	19	
GN-4-7	30	14	57.1
GH-4-7	72	22	

Table 10.
Effect of Concrete Compressive Strength on Ductility

Specimen	ρ	Δ_u/Δ_c	Decreasing %
GN-1-5	0.0048	16	18.75
GN-4-5	0.012	13	
GN-1-7	0.0048	14	0
GN-4-7	0.012	14	
GH-1-5	0.0048	22	27.2
GH-4-5	0.012	16	
GH-1-7	0.0048	26	26.9
GH-4-7	0.012	22	

5. CONCLUSIONS

The results of twenty specimens tested in this study, to investigate and assess the behavior of the GFRP bars as a replacement for the traditional steel reinforcement in eccentrically loaded walls, were discussed and the main outcomes can be stated as below.

1. In walls subjected to eccentric load, GFRP reinforcing bars act like steel ones regarding their effects on the mode of failure and the crack patterns.
2. Steel reinforced walls show 20% higher ultimate load than corresponding GFRP reinforced walls.
3. The ultimate load capacity increases with the addition of GFRP reinforcement, the ultimate load was increased by average 69.6 and 92.5% for NSC and HSC walls, respectively.
4. When ($f'c$) increased from 30 to 72 MPa the ultimate load in walls with 50 mm thickness increased by average 102.1, and by average 76.1% for walls with 70 mm thickness.
5. The behaviors of the GFRP reinforced specimens under load are similar to those of steel reinforced specimens with no distinguished plastic plateau.
6. The ductility of the specimen reinforced with GFRP bars is 60% higher than that of steel reinforced specimens of 50 mm thickness and 40% more for those of 70 mm.
7. The ductility of GFRP specimens decreases with the increase of reinforcement ratio by (average 9.4 and 27.1%) for NSC and HSC walls, respectively.

6. ABBREVIATIONS

GFRP Glass fiber reinforced polymer
NSC Normal strength concrete
HSC High strength concrete
P_c First crack applied load
P_u Ultimate applied load
Δ_c Deflection at first crack load
Δ_u Deflection at ultimate load
μ_u Ductility Index

REFERENCES

[1] ACI Committee 440'2006' Guide for the Design and Construction of Concrete Reinforced with FRP Bars (ACI 440. 1R -06), American Concrete Institute, Farmington Hill, MI, 44.

[2] Merritt F. S. and Ricketts J. T. (2000). Building design and construction hand book McGRAW-HILL, Sixth Edition, 11.41.

[3] Doh, J. H. (2002). Experimental and theoretical studies of normal and high strength concrete wall panel, Ph.D. Thesis – Griffith University, Cold Coast Campus.

[4] Benayoune, A.; Samad, A.A.A.; Trikha, D.N.; Abang Ali, A.A.; Ashrabov, A.A. (2006). Structural behaviour of eccentrically loaded precast sandwich panels. *Journal of Construction and Building Materials, 20*, 713–724.

[5] Swartz, S. E.; Rosebraugh, V. H.; Berman, M.Y. (1974). Buckling tests on rectangular concrete panels. *ACI Structural Journal, 71*, 33–39.

[6] Shah, Surendra P., Vijay Rangan, B., (1970). Effect of Reinforcements on Ductility of Concrete, *ASCE Proceedings, 96, ST6*.

[7] Lesile, K. E., Rajagopulan, K.S. and Everad, N.J., (1976). Flexural Behavior of High Strength Concrete Beams, *ACI Journal 73*(9), 517–521.

[8] Wang, P.T., Shah, S.P., and Naaman, A.E., (1978). High Strength Concrete in Ultimate Strength Design, *ASCE Journal of the Structure Division, 104*, 1761–1773.

[9] Elgabbas F., Vincent P., Ahmed E., Benmokrane B. (2016). Experimental Testing of Basalt-Fiber-Reinforced Polymer Bars in Concrete Beams. *Composites Part B: Engineering, 91*, 205–18.